

Nonlinear Growth in GaAs Molecular Beam Epitaxy

Anders Ballestad¹, Bayo Lau, Jens H. Schmid and Tom Tiedje²

Advanced Material and Process Engineering Laboratory, Department of Physics and Astronomy, University of British Columbia, Vancouver, BC, V6T 1Z4

¹anders@physics.ubc.ca, ²also Department of Electrical and Computer Engineering

ABSTRACT

We investigate experimentally and computationally the nonlinear replication of surface shapes during epitaxial growth. Experimental measurements of surface shapes consisting of atomic force microscope (AFM) images of epitaxially grown GaAs are compared with surface shapes computed from continuum growth equations with a conservative or a non-conservative nonlinear term. Both the non-conservative and the conservative nonlinear terms are found to be consistent with the experiments, although the conservative nonlinearity is preferred on physical grounds. Kinetic Monte Carlo (KMC) simulations cover a wider range of spatial frequencies, which enables the two different nonlinear terms to be distinguished. In this case, the observed surface shapes are consistent with the conservative nonlinearity.

INTRODUCTION

Regrowth on patterned semiconductor substrates is important in the fabrication of optical devices. An improved understanding of how surface shapes evolve during growth may create opportunities to improve control over the grown structures, including better lateral pattern definition as well as provide information on microscopic growth phenomena. Continuum equations are commonly used to model the morphology of surfaces during thin film deposition [1]. A random driving term is included in the growth equation to simulate the random arrival of atoms from the vapour, which leads to the kinetic roughening phenomenon. The scaling behaviour of the interface width as a function of time and surface area has been worked out theoretically and computationally for a variety of growth equations that are consistent with the required symmetries [1,2]. Experiments designed to determine which growth equation describes the system of interest typically involve measuring the scaling parameters for the interface width as a function of time and spatial frequency and comparing these values with theoretical values. If the scaling parameters obtained from the experimental data match the theoretical values for one of the growth equations, then one can conclude that this equation describes the experimental system of interest.

Two widely used growth equations are the KPZ and the MBE equations [1]:

$$\frac{\partial h}{\partial t} = \nu \nabla^2 h + \frac{\lambda}{2} (\nabla h)^2 + \eta \quad (\text{KPZ}) \quad (1)$$

$$\frac{\partial h}{\partial t} = -\kappa \nabla^4 h - \frac{\Lambda}{2} \nabla^2 (\nabla h)^2 + \eta \quad (\text{MBE}) \quad (2)$$

where $h(x,t)$ is the surface height and $\eta(x,t)$ is the noise associated with the random arrival of atoms. The coefficients in the equations arise from the underlying physical phenomena on the surface during growth. The growth equations are assumed to be in the moving frame of

reference for an average growth rate, F , and are valid in the limit of low amplitude, low spatial frequency surface topography.

Both equations 1 and 2 are nonlinear, but the nonlinearity in the MBE equation is conservative and in the KPZ equation it is non-conservative. In this context, non-conservative means that the surface topography contributes to the average growth rate. Also, the right hand side of equation 1 cannot be written as the divergence of a surface current. Both terms in the KPZ equation are second order in the spatial derivatives, while in the MBE equation they are both fourth order in the spatial derivatives. Terms of different order are not normally combined in growth equations as the higher order terms can be neglected at large length scales or small spatial frequencies (“hydrodynamic limit”) [2]. In this case the higher order terms are referred to as irrelevant. As the name suggests, irrelevant terms are not of much interest from a scaling perspective. However, there is no reason why they should not be important in real systems in a particular range of spatial frequencies. We show below that certain growth systems are better represented using an equation with an irrelevant term.

EXPERIMENTAL RESULTS AND CONTINUUM GROWTH EQUATIONS

A great deal is known about epitaxial growth of GaAs by molecular beam epitaxy, and as a result, it is a good system for testing growth models. In order to understand the shape evolution of GaAs surfaces quantitatively, we proceed by comparing the predictions of the growth equations with the shape and power spectral densities of the surfaces of the grown epitaxial films.

Comparison of experimental measurements of the surface morphology of GaAs layers grown on substrates with low amplitude surface roughness, show good agreement with numerical solutions of the KPZ equation, but poor agreement with the MBE equation [3]. This is surprising since the deposited layers were grown in the regime where all of the deposited Ga atoms stick to the surface and the growth equation should be conservative. One might argue that there are higher order terms, which are neglected in the KPZ equation, that maintain conservative growth. Growth along the outward surface normal is the usual explanation for the KPZ nonlinearity. Earlier, we suggested that this might happen if the growth took place from a highly mobile surface adatom layer, which could act as a 2D gas phase. In this case, the coefficient λ of the nonlinear term in the KPZ equation should be equal to the growth rate. However, growth simulations show that the nonlinearity is much bigger than this and requires a λ value that is more than an order of magnitude larger than the growth rate F [3].

Another possibility is that the nonlinearity is not a geometrical effect associated with growth along the outward normal and that it has a different origin. We consider instead a mixed-order conservative equation that combines the linear term from the KPZ equation with the nonlinear term from the MBE equation:

$$\frac{\partial h}{\partial t} = \nu \nabla^2 h - \frac{\Lambda}{2} \nabla^2 (\nabla h)^2 + \eta \quad (3)$$

In this case, the nonlinear term has a different microscopic origin and there is no requirement that the coefficient of the nonlinear term be equal to the growth rate. In practice, if the surface morphology is only measured over a small spatial frequency range, and the coefficient of the nonlinear term is not too large, the two different nonlinear terms may be difficult to distinguish

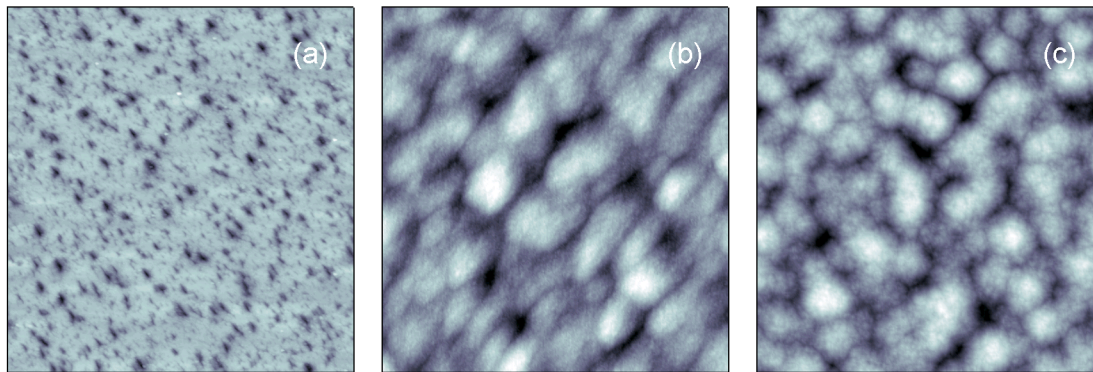


Figure 1. GaAs epitaxy on random surfaces: (a) AFM image of thermally desorbed starting surface (z-range 50 nm); (b) AFM image after 90 minutes of growth at 0.8 ML/s (z-range 6 nm); (c) simulated image based on equation 3 (z-range 6 nm). Image sizes are $10 \times 10 \mu\text{m}$.

experimentally.

Figure 1b shows an AFM image of a $1.2 \mu\text{m}$ thick GaAs epitaxial layer deposited on a thermally cleaned substrate, such as that shown in figure 1a. As discussed elsewhere, the mounds observed in this image result from incomplete smoothing of the surface roughness produced during the thermal desorption of the surface oxide [3,4]. The surface morphology can be characterized as consisting of smoothly rounded mounds separated by v-shaped valleys. This surface lacks inversion symmetry, which means that the growth equation must be nonlinear. A numerical simulation of the surface structure using equation 3 is shown in figure 1c using the method discussed earlier [3]. The simulated surface morphology was computed using the AFM image of a thermally cleaned GaAs substrate as the initial condition.

The power spectral density for this surface is shown in figure 2, along with the power spectral densities computed from the simulated surface structures using equations 1 and 3. The characteristic length (peak in PSD) is associated with the spacing of the pits on the starting surface. In the KPZ simulation (figure 2a), we used non-conservative noise and $\nu_x = 10 \text{ nm}^2/\text{s}$, $\nu_y = 1 \text{ nm}^2/\text{s}$ and $\lambda = 12 \text{ nm}/\text{s}$, where the x is in the $[1\bar{1}0]$ direction and y is the $[110]$ direction. The amplitude of the noise was adjusted to match the power spectral density at high spatial frequency. In the simulation of equation 3 (figure 2b), we also used non-conservative noise and the parameters $\nu_x = 10 \text{ nm}^2/\text{s}$, $\nu_y = 1 \text{ nm}^2/\text{s}$ and $\Lambda = 10^6 \text{ nm}^3/\text{s}$. We can compare the relative magnitudes of the conservative and non-conservative nonlinear terms in equations 1 and 3, at a given spatial frequency q , by replacing the gradient operators by q . If we take $q = 3 \mu\text{m}^{-1}$ as a typical q value in the range where the nonlinear term is important, then we would expect $\lambda = q^2 \Lambda = 9 \text{ nm}/\text{s}$. This agrees well with the KPZ simulation, where we used $\lambda = 12 \text{ nm}/\text{s}$. As pointed out earlier, λ is much larger than the growth rate, which is about $0.3 \text{ nm}/\text{s}$ in these experiments. If the correct nonlinear term were the conservative fourth order term in equation 3, then one would not expect λ determined from a fit to the KPZ equation to have any relationship to the growth rate.

The spatial frequency range obtained experimentally from AFM images can be expected to be accurate over less than two orders of magnitude. The low spatial frequency limit is set by the size of the imaged area and the resolution of the AFM, and the number of pixels in the image and the size of the AFM tip set the upper spatial frequency limit. In the experimentally accessible

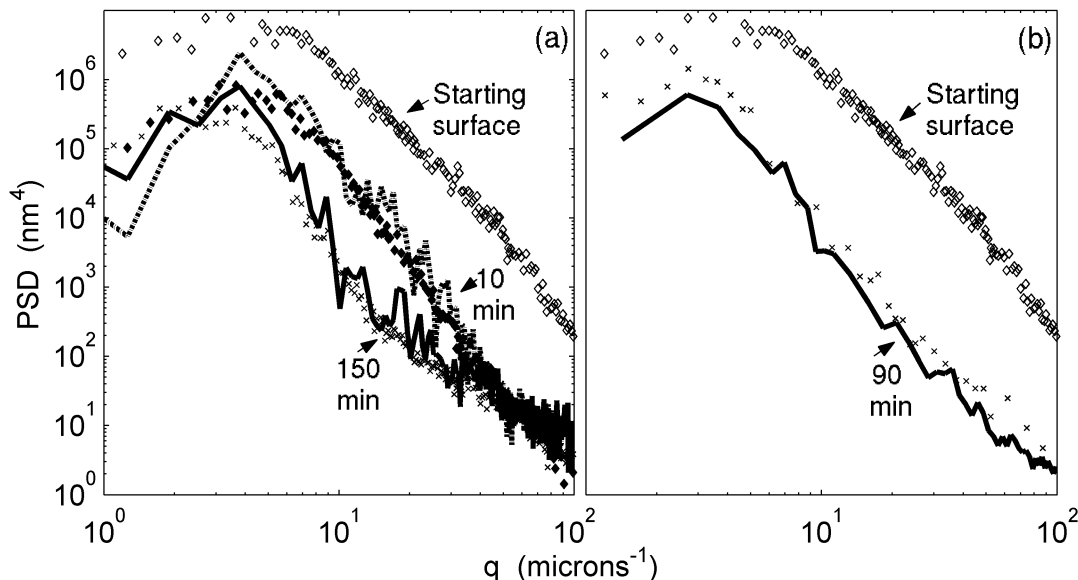


Figure 2. Power spectral density along [110] direction for epitaxial GaAs films grown on random surfaces. (a) The symbols are experimental data for the starting surface (top), after 10 min of growth (middle) and 150 minutes of growth (bottom) for a 1 ML/s growth rate. KPZ simulations are indicated by the dotted and solid lines, according to 10 and 150 min of growth, respectively. (b) The experimental data for the starting surface is the same (top) along with data after 90 minutes of growth at 0.8 ML/s (bottom). The solid line is a simulation using equation 3. Substrate temperature was 550°C for all growths. The power spectral densities for spatial frequencies less than $\sim 2 \mu\text{m}^{-1}$ are not considered to be reliable.

spatial frequency range, the KPZ equation (1) and the mixed-order equation 3 give similarly good fits to the measured power spectral density for the GaAs surface. Qualitatively, both equations produce a mounded surface morphology with v-shaped valleys, however, the experimental data is not sufficiently precise to allow us to choose between the two nonlinear terms. Physically, equation 3 is more appealing as it is conservative, which is consistent with the MBE growth process.

SOLID ON SOLID MODEL SIMULATIONS

The continuum growth equations can also be compared with kinetic Monte Carlo (KMC) simulations of a solid-on-solid (SOS) model. These simulations are computational experiments in which all of the microscopic “physical” phenomena are known. We use a square grid and a mono-atomic crystal. Adatoms are free to hop on the square lattice, attach and detach from existing islands, or nucleate with other diffusing adatoms and form monolayer islands. Each atom bonds to the surface with an activation energy $E_{act} = E_{sub} + mE_{lat}$, where m is the number of lateral nearest neighbors. The parameters used in the simulations were: $E_{sub} = 1.25$ eV, $E_{lat} = 0.35$ eV, $F = 1$ ML/s and $T = 575^\circ\text{C}$. The SOS model is restricted, in the sense that double height steps are not allowed. To incorporate a second order KPZ-type linear term in the growth equation, we include a step-edge potential barrier that favours downhill adatom migration. This is the so-called *inverse* Ehrlich-Schwoebel barrier. While it remains unclear exactly what the magnitude of this barrier is in the case of GaAs, it is clear that the surface tends to smooth, and that a net downhill adatom drift mechanism is necessary in order to explain the experimental data. This could also be achieved by incorporating the effects of downhill funneling [5], or the

knock-out effect [1]. However, these are both non-equilibrium effects that cannot explain the continued smoothing that is observed during annealing [6]. For simplicity, we use a negative ES barrier (attractive step edge potential) of magnitude $E_{ES} = -0.05$ eV in order to describe the experimentally observed bias at the step-edge. This choice might seem counter-intuitive, however, considering the repeated experimental indication that the net direction of adatom drift is downhill, such a choice constitutes the simplest explanation to interlayer transport in this material system both during growth and annealing [2,3,6]. The simulation is carried out on a 600×600 lattice with a 1D sinusoidal surface topography as the initial condition [6]. Cross-sectional scan lines from the simulations are shown in figure 3. The scan lines are projections of the average surface height along the 2D surface parallel to the gratings.

Three different sinusoidal topographies were used as initial conditions with different amplitudes and spatial frequencies, as shown in figure 3. The choice of starting conditions is designed to illustrate the effects of amplitude and spatial frequency on the shape of the surface during growth. Figure 3a-c show the surface cross sections after depositing 0, 30, 60, and 90 monolayers of material. The first panel (a) shows the topography for the long wavelength, low amplitude starting surface. This surface shows a relatively weak nonlinear growth as indicated by the slightly v-shaped valleys for the thickest deposited layers. The second panel (b) shows the effect of doubling the spatial frequency. As expected, the amplitude of the topography decays faster in the second panel, since in the Fourier domain both the linear and nonlinear terms on the right hand side of the growth equations increase with spatial frequency as $\sim q^2$ due to the gradient operators. In addition, growth on the short period grating is significantly more nonlinear than for the longer period grating, and v-shaped valleys form after a relatively small decay in amplitude. If one doubles the spatial frequency of the surface, the amplitude of both the linear term and the nonlinear term in the KPZ equation increases by a factor of four. If one rescales

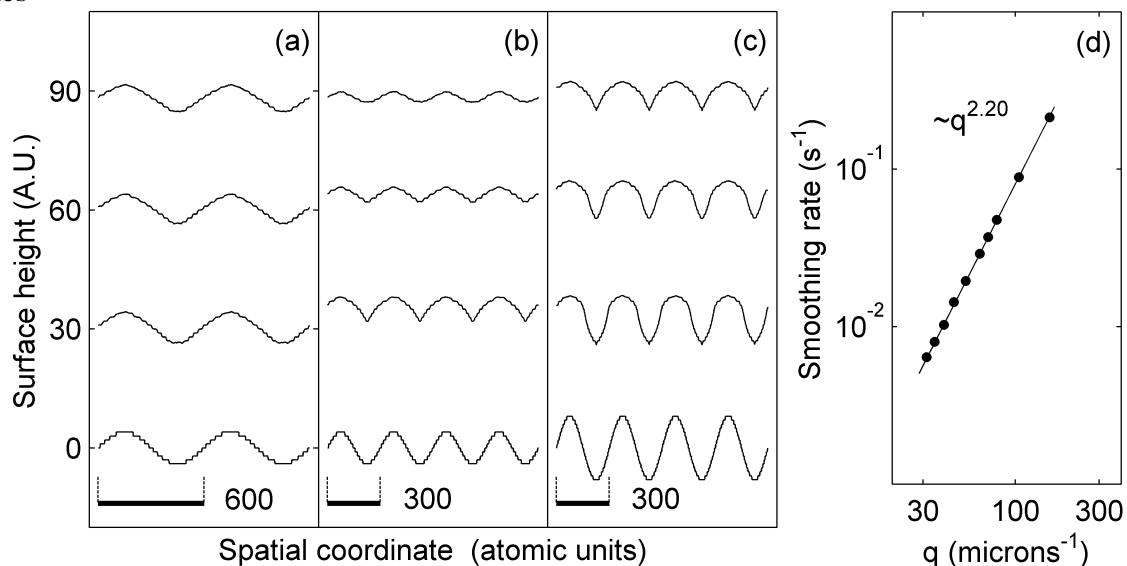


Figure 3. Effect of spatial frequency and amplitude of surface topography on surface evolution. Projected 2D SOS simulations with three different sinusoidal initial topographies: (a) 600 atom period, 4 atom amplitude (*i.e.* 9 discrete atomic levels); (b) 300 atom period, 4 atom amplitude; and (c) 300 atom period, 8 atom amplitude. Part (d) shows the smoothing rate as a function of the pitch (or spatial frequency) of low amplitude gratings similar to (a). An atom diameter is assumed to be 0.3 nm.

the time by a factor of four to take into account the faster decay rate the surface shape evolution will be the same. However, the simulation shows that the relative importance of the nonlinearity increases when the spatial frequency is increased. This result is inconsistent with the KPZ equation but consistent with equation 3, where the ratio of the nonlinear term to the linear term increases by a factor of four if the spatial frequency is doubled. Therefore, the KMC simulations are qualitatively consistent with equation 3. The third panel, figure 3c, shows that doubling both the amplitude and the spatial frequency of the starting surface produces a rather complex nonlinear distortion of the surface in addition to v-shaped valleys. This may be an indication that the description of the growth in terms of asymptotic growth equations is breaking down for the relatively large surface gradients in figure 3c.

From theoretical considerations, we expect the negative step edge barrier in the SOS simulations to produce a second-order linear term in the growth equation, similar to equations 1 and 3 [7]. To test this prediction, KMC simulations were performed on a series of sinusoidal starting surfaces with different spatial frequencies. The smoothing rate of the different surfaces is plotted on a log-scale in figure 3d as a function of spatial frequency. We determined the smoothing rate by fitting an exponential to the RMS surface height as a function of growth time. The best-fit line shows a $q^{2.2}$ dependence on spatial frequency. This is close to the q^2 dependence expected for smoothing with a second order linear term. Since the non-linear term will also contribute to surface smoothing some deviation from q^2 can be anticipated.

CONCLUSIONS

In conclusion, kinetic Monte Carlo simulations of surface shapes during film growth on patterned substrates with negative Ehrlich-Schwoebel barriers are compared with a description based on continuum growth equations. The KMC simulations are consistent with a continuum growth equation in which the linear term is second order in the spatial derivative $(\nabla h)^2$ and the nonlinear term is fourth order in the spatial derivative $(\nabla^2(\nabla h))^2$. This mixed order growth equation is also consistent with experimental atomic force microscopy images of GaAs epitaxial layers grown on substrates with a random initial surface topography. However, the spatial frequency range of the experimental data for the GaAs surfaces is not sufficiently large to distinguish the fourth order nonlinear term from the second order one. Since the GaAs growth is conservative, the conservative fourth order nonlinear term is more appealing physically than the second order nonlinear term, which is non-conservative.

REFERENCES

1. A. Pimpinelli, J. Villain, *Physics of Crystal Growth*, Cambridge U. Press (1998).
2. J. Krug, *Adv. Phys.* **46**, 139-282, (1997).
3. A. Ballestad, B. J. Ruck, J. H. Schmid, M. Adamcyk, E. Nodwell, C. Nicoll and T. Tiedje, *Phys. Rev. B* **65**, 205302 (2002).
4. A. Ballestad, B. J. Ruck, M. Adamcyk, T. Pinnington and T. Tiedje, *Phys. Rev. Lett.* **86**, 2377 (2001).
5. P. Smilauer and D. Vvedensky, *Phys. Rev. B* **48**, 17603 (1993).
6. A. Ballestad, T. Tiedje, J. H. Schmid, B. J. Ruck and M. Adamcyk, *J. Cryst. Growth* **271**, 13-21 (2004).
7. J. Villain, *J. de Physique I* **1**, 19 (1991).